Supplementary information for "Bi-Analyte Single Molecule SERS with Simultaneous Spatial Resolution"

Determination of the spatial resolution of the CCD

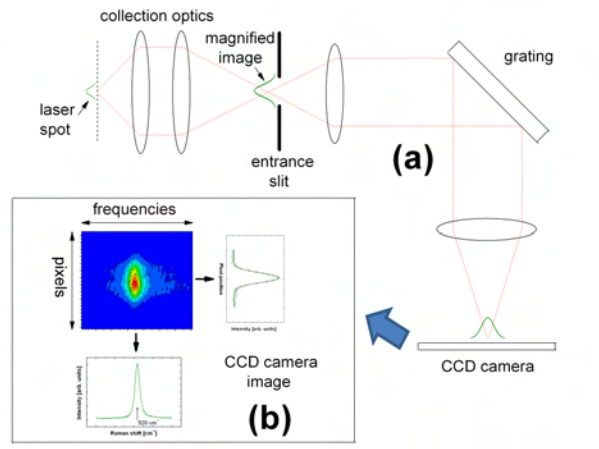

FIG. S1: (a) Schematic representation of the spectrometer. The laser spot on the sample is amplified by a fixed magnification factor of the collecting optics onto the entrance slit of the spectrometer; which in our machine is the same as the confocal pinhole and it is computer controlled. The magnification of the collecting optics in our system for a $\times 100$ objective is $X = 56$. The Raman signal on Si is studied as a function of the pinhole (entrance slit) size, following the protocols developed in the supplementary information of Ref. [1]. The Raman signal in this case is proportional to the area of the spot that is being allowed through at the entrance slit. In (b) we show the result of analyzing the CCD image by projecting (integrating) the signal along the frequency or spatial dimensions. The signal projected on the frequency dimension is the standard Raman spectrum with a width (in pixels) decided by the dispersion of the grating. The signal projected on the spatial dimension, on the other hand, has information on the actual size of the magnified beam on the entrance slit (in the direction parallel to the grooves of the grating). This information is, however, somewhat convoluted by the astigmatic spread of the spectrometer. See the text for further details.

The determination of the spatial resolution on the CCD is not straightforward for a variety of reasons that will be explained in more detail here to complement the information on the main paper. Initially, we characterize the Gaussian beam profile of the laser on the sample. This is a required step to understand the final image produced on the CCD. The characterization of the beam waist of the Gaussian excitation profile on the sample is done by following the protocol developed in full in the supplementary information of Ref. [1] (see also the supplementary information of Ref. [2] for further examples). We summarize here briefly the main points. Essentially, we study the variation of the Raman signal of Si as a function of the confocal pinhole size; which in our machine (Jobin Yvon LabRam UV/Visible) is the same as the entrance slit. In Fig. S1(a) we represent schematically the optical layout. For a $\times 100$ objective used in collection, the laser spot is magnified by a factor of $X = 56$ onto the entrance (confocal) slit of the spectrometer. The latter is square-shaped and can be computer controlled in the range $0-1000\,\mu$m (diagonal size). By studying the variation of the Raman signal as a function of the pinhole size –and fitting the result to an error function (the integral of a Gaussian)– it is possible to measure the beam waist of the laser spot (w_0). The spot itself on the sample can be well represented by a Gaussian intensity profile of the type [1]:

$$I(\rho) = I_0 \exp\left(-\frac{2\rho^2}{w_0^2}\right), \tag{S1}$$

where I_0 is the power density at the centre, and ρ is the radial direction on the focal plane of the sample (measured from the beam center). I_0 [W/m^2] is related to the power P_0 [W] in the beam through the beam waist w_0 [m] via $P_0 = (\pi w_0^2 I_0/2)$ [1]. Note that w_0 is the radial distance at which the intensity of the Gaussian beam has decreased to $\exp(-2) \sim 13\%$ of the intensity at the top. The actual fit to an error function of the experimental data is more complicated in reality, because one normally allows for a small offset (x_0, y_0) in the alignment of the beam; thus resulting in a fit with three independent parameters: x_0, y_0, and w_0 (see Eq. S37 in the supplementary information of Ref. [1]). It is normally a prerequisite that the beam is aligned as perfect as possible with the optical axis of the instrument to perform the slit scan. From there, w_0 can be obtained through the magnification of the collecting optics (X). This method of determining the beam waist of the laser is based on well established knife-edge techniques for beam profiling [3], with the only proviso that it is done here through the Raman signal rather than the intensiy of the laser itself.

An important point is the following: in this initial stage, the Raman signal on the CCD (Fig. S1(b)) is not analyzed in its details at all; the whole signal is integrated with the appropriate binning of the CCD in both the spatial and frequency dimensions, and it only represents a signal *proportional* to the area of the beam being allowed through at the entrance (confocal) slit. The signal on the CCD itself can be deformed or distorted by aberrations or imperfections, but it is still a

valid measure of the total intensity for as long as all the signal is integrated with an appropriate binning of the CCD. Typical values of w_0 obtained with this method are a fraction of the wavelength being used (λ) for diffraction limited spots achieved with high numerical aperture objectives (like $\times$100, NA=0.9). A much more difficult problem is to interpret the exact image on the CCD, which is our next task. This is required if simultaneous spatial and frequency information is sought.

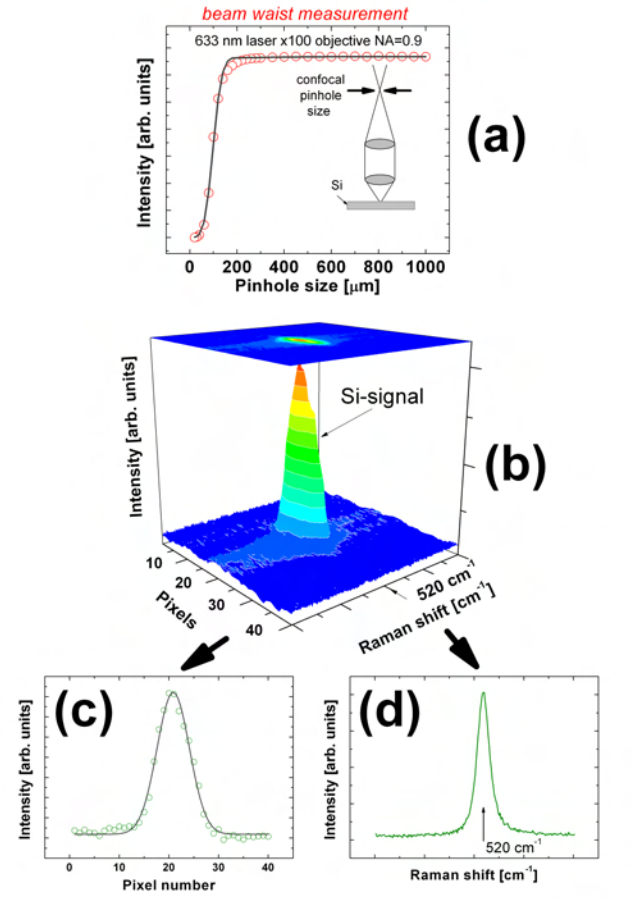

FIG. S2: (a) Beam waist (w_0) characterization using the confocal pinhole dependence [1, 2] of the 520 cm^{-1} Raman mode of Si. From a fit of the the pinhole dependence (red line) we obtain $w_0 = 460$ nm. This implies a magnified beam at the entrance slit with a waist of $Xw_0 = 25.8\,\mu$m, which is imaged after going through the grating onto the CCD as shown in (b). The projected (integrated) signal in the frequency dimension provides the Gaussian spatial profile in (c), while (d) shows the standard Raman signal of Si (at 520 cm^{-1}) projected (integrated) along the spatial dimension axis. From a Gaussian fit to the data in (c) and the determination of w_0 from (a), we could obtain the conversion factor $K = w_0/w_p$ between pixels and real dimensions. The spatial dimension, however, is affected by the presence of astigmatism, as explain further in Figs. S3 and S4.

To analyze the image on the CCD, we start first with the description of the idealized case, and then develop further the interpretation to account for the presence of astigmatism. The idealized situation could be described as follows: Once w_0 is known, it is also known that a magnified version of the Gaussian intensity distribution on the sample exists on the entrance slit (with a magnified beam waist = Xw_0). The spectrometer itself (internally) has a magnification = 1 between the entrance slit and the image on the CCD. The image of the Raman peak on the CCD can now be analyzed in more detail, as shown schematically in Fig. S1(b). The image has basically two dimensions: the spatial one (parallel to the grooves on the grating), and the frequency one (perpendicular to the grooves). In the frequency dimension, the image will spread over a distance (in pixels) which is fixed by the dispersion of the grating. The signal integrated in the spatial direction –for different pixels in the frequency axis– is what is normally measured in the spectrometer as "the Raman peak". On the other hand, the signal integrated in the frequency direction –for different pixels in the spatial dimension– reveals a profile that comes, in principle, from the magnified version of the laser spot on the entrance slit, in the direction parallel to the grooves of the grating. In the spatial direction of the CCD the spectrometer behaves basically as an imaging microscope, subject to the standards constraints of the diffraction limit and image aberrations [4]. This is schematically represented in Fig. S1(b).

However, a *bona fide* estimation of the beam size on the CCD reveals that there is a problem. The Gaussian profile of the spot on the CCD (integrated in the frequency dimension) can be fitted to:

$$I(p) = A \exp\left(-\frac{2(p-p_0)^2}{w_p^2}\right), \qquad \text{(S2)}$$

where A is a constant, p is the pixel number, p_0 is the central pixel, and w_p is the beam waist in pixel units. In principle, w_0 in real (distance) units should correspond to w_p in pixel units under perfect imaging conditions. From here, we could immediately obtain the conversion factor $K = w_0/w_p$ between pixels and real dimensions on the spot.

Figure S2 shows an actual measurement for our system. In Fig. S2(a) we show the beam waist characterization [1, 2] using the entrance (confocal) pinhole (from where we obtain $w_0 = 460$ nm), while Figs. S2(b-d) show the CCD image with its projected (integrated) signals in the spatial and frequency dimensions. From the fit to w_0 in Fig. S2(a) and that to w_p in Fig. S2(c), we could obtain –in principle– the conversion factor $K = w_0/w_p$. However, there is a problem with this value and that can be appreciated from the fact that the

real (physical) pixel size of our CCD is $26\,\mu\text{m} \times 26\,\mu\text{m}$ according to factory specifications. If the original beam on the sample has a waist of $w_0 = 460\,\text{nm}$ (determined by the knife-edge profiling in the previous step) and it is magnified by a factor of $X = 56$ on the entrance slit, then most of the beam should be contained within a radius of $\sim 25\,\mu\text{m}$; i.e. $\sim 1-2$ pixels (perhaps $\sim 3-4$ if a bit of inter-pixel spreading is allowed). But this is not what happens in Fig. S2(b), and the main reason for this is astigmatism [4].

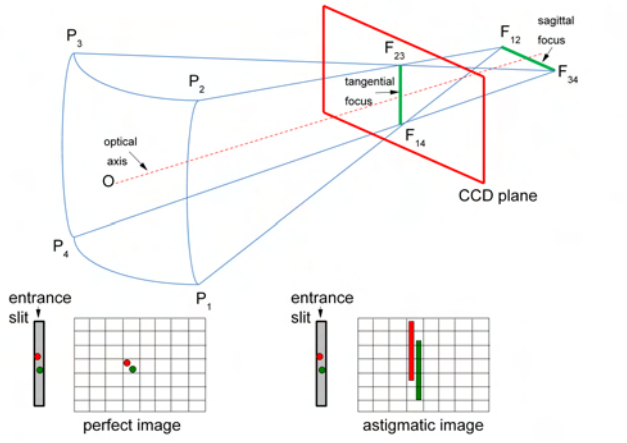

FIG. S3: Astigmatism is produced by the different curvature of the optics in different directions (here exemplified by a simple collecting mirror). The tangential (sagittal) focal plane produces an astigmatism-free image in the horizontal (vertical) direction. In normal spectrometers, the optics is optimized for the CCD plane to be at the tangential focus. In a perfect situation, point-like sources at the entrance slit will be imaged into equivalent points on the CCD plane. However, under the presence of astigmatism, point-like sources are imaged into vertical lines at the tangential focal plane of the CCD. These two examples are shown schematically at the bottom. See Ref. [5] for further details.

Unless one works with special spectrometers with toroidal optics [5] (or aberration-corrected prism spectrometers, like the PARISS spectrometer [5] used in fluorescence) most spectrometers will be optimized to compensate for astigmatism at the tangential focal plane, as depicted in Fig. S3. This is because the horizontal axis is the one containing the spectral information, and we do not want any additional instrumental blurring on that axis (except for the one produced by the natural linewidth of a peak, the dispersion of the grating, the slits setting, and the finite size of the imaged object). The presence of astigmatism in the vertical axis is not much of a problem under normal circumstances, for typically we will be integrating several lines of diodes on the CCD along the vertical direction with an appropriate binning. Therefore, under the normal operating mode of the spectrometer astigmatism is automatically accounted for and is pushed into a dimension where it is not a problem. Nevertheless, it does become a matter of concern if we want to retrieve both spatial as well as spectral information simultaneously.

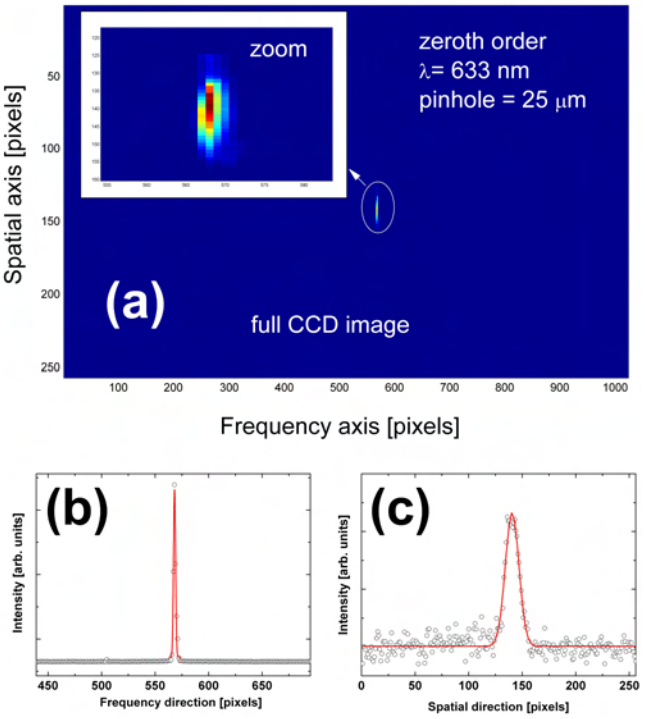

FIG. S4: Experiment to show the presence of astigmatism. The image of the attenuated laser (633 nm) through an entrance slit of $25\,\mu\text{m}$ is taken on the CCD with the grating at zeroth-order (i.e. working as an imaging device). Under ideal conditions, most of the image on the CCD should be contained within $\sim 1-2$ pixels in both horizontal and vertical directions. However, the vertical spread of the image in (a) is ~ 8 times larger in the vertical (spatial) direction than in the horizontal (frequency) one. This can be quantified by looking at the projections of the signal on both axes, as shown in (b) and (c). The CCD is at the tangential plane and the astigmatic spread is more pronounced in the vertical direction.

In order to demonstrate that there is indeed an astigmatic spread in the vertical (spatial) direction, the following experiment was carried out: The laser was carefully aligned to hit the entrance slit in the middle and this was set to a size of $25\,\mu\text{m}$. The grating is set at its zeroth order (reflection) and an image of the entrance slit is obtained. The spectrometer works in this case as an "imaging device" and with an internal magnification =1 we expect most of the image to be concentrated within 1-2 pixels (3-4 with some inter-pixel blurring) in both directions. Fig. S4(a) reveals that the image of the entrance slit is indeed concentrated (mostly) on one central pixel in the horizontal direction, but it is eight times more spread out in the vertical axis. This

can be directly quantified by looking at the (integrated) projections of the signal along both axes, as shown in Figs. S4(b) and (c).

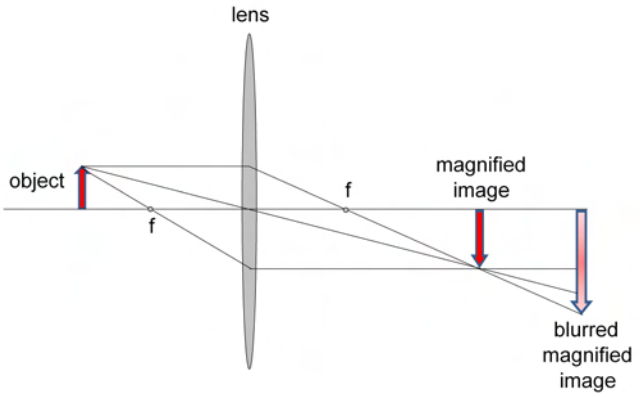

FIG. S5: Magnification with blurring outside the normal focal plane does not result in an increased spatial resolution. We exemplify this here with the example of a simple imaging system consisting of one lens. Each point in the blurred image beyond the image plane has a *point spread function*, exactly like the one that appears through other aberrations (like astigmatism). Even though when the image is magnified and a connection can be made with the original image, it does not result in an increased ability to resolve spatial details. Moreover, single points in the image make contributions to multiple point in the defocused one, thus resulting in the blurring of spatial information.

The result in Fig. S4, however, can still be affected by the finite size of the image on the entrance slit, and this is where it becomes interesting to know what the astigmatic spread would be for an ideal point-like source. But this is, indeed, one of the answers one can get by looking at signals from single molecules. From an experimental point of view, we can claim SM-spectra to be the best possible realization of a point-like source. In fact, this is a possible application of SM-spectroscopy, namely: the experimental realization of point-like emitters to analyze fundamental aspects of the optics of instruments. The width of SM-events in the spatial dimension define the so-called *astigmatic point spread function* (APSF) of the instrument. By looking at different SM-events in the spatial dimension of the CCD in Fig. 3(d) of the main paper we see that the APSF has typical widths in the range of 7-pixels. The illumination profile of the laser (which should have been contained within 1-2 pixels under ideal conditions) is convoluted with the APSF and it obviously dominated by it. Indeed, Fig. 3(d) of the main paper shows that the illumination envelope on a Si sample can accommodate $\sim 1-1.5$ SM-events in the spatial dimension. Therefore, this increase in size by blurring should not be considered as a magnification when we are trying to relate distances on the CCD image plane with distances on the real sample. This is, in fact, the case for any optical image with aberrations (including plain ones, like defocusing, as shown schematically in Fig. S5).

The presence of a "natural spread" from the APSF implies in practice for our case that if peaks happen at exactly the same frequency (horizontal axis) they need to be separated by (at least) 4 pixels to be distinguishable as two separate peaks. This implies a size of $\sim 100\,\mu$m on the CCD (taking the pixel size as $\sim 25\,\mu$m; i.e. $\sim 1.7\,\mu$m on the real sample (after demagnification by a factor of $X = 56$). If the peaks are *not* at the same frequency, as it happens in some mixed events, they can be distinguished in the spatial axis within a single pixel (i.e. $\sim 450\,$nm, in the best of cases). Simultaneous peaks at the same frequency can appear as far apart as $\sim 10-15$ pixels, which represents distances of the order of $\sim 4-5\,\mu$m. In any case, all these estimations give values well above the diffraction limit which is $\sim 380\,$nm for $\lambda = 633\,$nm. Therefore, there is no super-resolution here, or similar claims that have been made for SM-SERS [6]. The only claim here is the experimental fact that we observe SM-events that are spatially resolved, and that those would have been "integrated" and mingled by the CCD binning in the standard implementation of the bi-analyte SERS technique. Here, however, we gain an additional insight into the origin of the signals, including the presence of different molecules at slightly different frequencies (contributing to the inhomogeneous broadening of the peaks [7]), and the existence of Surface-Enhanced Fluorescence (SEF) backgrounds that can be traced back to individual single molecules.

A final question remains though, and this is related to the experimental fact that SM-SERS events can be observed as far apart as $\sim 4-5\,\mu$m. This comes indeed from an additional effect present in our experiments: the perturbation of the beam illumination by the presence of metallic clusters in the sample. It turns out that a beam waist characterization like that in Fig. S2(a) but done on top of colloidal clusters reveals perturbations in the tail of the beam that go all the way to $\sim 400-700\,\mu$m (in confocal slit size). At $\sim 300\,\mu$m slit size, for example, we could easily have $\sim 10-20\%$ of the signal spread on the tail of the beam when it is focused on clusters. This, combined with the huge enhancements of some SERS hot-spots, makes it possible to observe SM-events that are separated as far apart as $\sim 5\,\mu$m on the sample (taking into account the magnification of $X = 56$). In fact, these are the examples that look normally *clearer* in the statistics, for the events are widely seraparated in the spatial dimension and they are easy to identify. It is interesting to note then that the events that show the clearest separation of SM-signals in the spatial

dimension are those in which the illumination comes (mainly) from an "unwanted" effect of spreading the beam by focusing on metallic clusters.

In summary, the spatial dimension of the CCD image contains contributions from the standard magnification of the collecting optics and the natural blurring of astigmatic aberrations. With some natural limitations, signals by single molecules can be spatially resolved and analyzed for their contributions to the overall signal in the bi-analyte method. The combination of spatial and spectral information opens a new dimension into the origin of many effects that are seen in single molecule SERS experiments.

[1] E. C. Le Ru, E. Blackie, M. Meyer, and P. G. Etchegoin, J. Phys. Chem. C **111**, 13794 (2007).

[2] J. E. Bohn, P. G. Etchegoin, E. C. Le Ru, R. Xiang, S. Chiashi, and S. Maruyama, ACS Nano **4**, 3466 (2010).

[3] W. Plass, R. Maestle, K. Wittig, A. Voss, and A. Giesen, Optics Communications **134**, 21 (1997).

[4] M. Born and E. Wolf, *Principles of Optics, 6*$^{\text{th}}$*-edition* (Pergamon Press Ltd., Oxford, 1980).

[5] J. M. Lerner, Cytometry, Part A **69A**, 712 (2006).

[6] S. M. Stranahan and K. A. Willets, Nano Lett. **10**, 3777 (2010).

[7] P. G. Etchegoin and E. C. Le Ru, Anal. Chem. **82**, 2888 (2010).